Supplementary Information (SI) for Inorganic Chemistry Frontiers.

Magnetic Dynamics and Exchange Coupling in Dinuclear Lanthanide Complexes Bridged by Naphthoquinone and Anthraquinone Radicals

Dimitris I. Alexandropoulos,*[a,b] Kuduva R. Vignesh, [a,c] Luís Cunha-Silva,[d] and Kim R. Dunbar*[a]

[a.] *Department of Chemistry, Texas A&M University, College Station, Texas 77842-3012, United States. Email: dunbar@chem.tamu.edu*

[b.] *Department of Chemistry, University of Patras, Patras 26504, Greece*

[c.] *Department of Chemical Sciences, Indian Institute of Science Education and Research (IISER) Mohali, Sector-81, Knowledge city, S.A.S. Nagar, Mohali-140306, Punjab, India.*

[d.] *LAQV/REQUIMTE & Department of Chemistry and Biochemistry, Faculty of Sciences, University of Porto, 4169-007 Porto, Portugal.*

Single-crystal X-ray crystallography

Table S1. Crystal data and structural refinement parameters for compounds **1**·6CH_2Cl_2, **2**·6CH_2Cl_2, **3**·2THF and **4**·2THF.

Identification code	**1**·6CH_2Cl_2	**2**·6CH_2Cl_2	**3**·2THF	**4**·2THF
Empirical formula	$C_{52}H_{56}B_4Cl_{12}Dy_2N_{24}O_4$	$C_{56}H_{58}B_4Cl_{12}Dy_2N_{24}O_4$	$C_{66}H_{84}B_4Dy_2KN_{24}O_{12}$	$C_{70}H_{110}B_4Dy_2KN_{24}O_{12}$
Formula weight	1874.84	1924.9	1812.91	1887.15
Temperature	110(2) K	110(2) K	110(2) K	110(2) K
Wavelength	0.71073 Å	0.71073 Å	0.71073 Å	0.71073 Å
Crystal system	Triclinic	Triclinic	Triclinic	Monoclinic
Space group	$P\bar{1}$	$P\bar{1}$	$P\bar{1}$	C2/c
Unit cell dimensions	a = 9.0886(7) Å	a = 9.225(5) Å	a = 13.143(13) Å	a = 19.3445(9) Å
	b = 12.9498(9) Å	b = 12.793(7) Å	b = 13.277(7) Å	b = 19.6804(10) Å
	c = 16.2560(11) Å	c = 17.023(9) Å	c = 13.592(8) Å	c = 24.9870(13) Å
	a= 83.661(2)°	a= 93.36(2T)°	a= 110.830(16)°	a= 90°
	b= 85.814(2)°	b= 90.838(13)°	b= 107.00(3)°	b= 111.716(2)°
	g = 70.718(2)°	g = 109.433(16)	g = 104.30(3)°	g = 90°
Volume	1793.5(2) Å^3	1890.0(17) Å^3	1950(3) Å^3	8837.6(8) Å^3
Z	1	1	1	4
Density (calculated)	1.736 Mg/m^3	1.691 Mg/m^3	1.544 Mg/m^3	1.418 Mg/m^3
Absorption coefficient	2.576 mm^{-1}	2.447 mm^{-1}	2.028 mm^{-1}	1.793 mm^{-1}
F(000)	924	950	915	3860
Crystal size	0.350 x 0.100 x 0.060 mm^3	0.500 x 0.100 x 0.080 mm^3	0.450 x 0.120 x 0.070 mm^3	0.400 x 0.110 x 0.040 mm^3
Theta range for data collection	3.671 to 25.778°	2.139 to 25.767°	3.686 to 25.026°	3.932 to 26.176°
Index ranges	-11<=h<=9	-11<=h<=11	-15<=h<=15	-23<=h<=23
	-15<=k<=15	-15<=k<=15	-15<=k<=15	-24<=k<=24
	-19<=l<=19	-20<=l<=20	-16<=l<=16	-30<=l<=30
Reflections collected	18708	55685	30198	30559
Independent reflections	6791 R(int) = 0.0472	7216 R(int) = 0.0547	6861 R(int) = 0.0787	8750 R(int) = 0.0417
Completeness to theta = 25.242°	99.20%	100.00%	99.60%	99.60%
Absorption correction	Semi-empirical from equivalents	Semi-empirical from equivalents	Semi-empirical from equivalents	Semi-empirical from equivalents
Max. and min. transmission	0.857 and 0.402	0.822 and 0.294	0.868 and 0.401	0.931 and 0.488
Refinement method	Full-matrix least-squares on F^2	Full-matrix least-squares on F^2	Full-matrix least-squares on F^2	Full-matrix least-squares on F^2

Data / restraints / parameters	6791 / 0 / 442	7216 / 0 / 460	6861 / 0 / 502	8750 / 0 / 546
Goodness-of-fit on F2	1.28	1.071	1.065	1.123
Final R indices	R_1 = 0.0484	R_1 = 0.0291	R_1 = 0.0853	R_1 = 0.0594
[I>2sigma(I)]	wR_2 = 0.1265	wR_2 = 0.0645	wR_2 = 0.2249	wR_2 = 0.1541
R indices (all data)	R_1[a] = 0.0495	R_1 = 0.0329	R_1 = 0.0988	R_1 = 0.0792
	wR_2[b] = 0.1271	wR_2 = 0.0664	wR_2 = 0.2409	wR_2 = 0.1669
Extinction coefficient	n/a	n/a	n/a	n/a
Largest diff. peak and hole	2.647 and -2.371 e.Å^{-3}	2.791 and -1.333 e.Å^{-3}	8.014 and -2.860 e.Å^{-3}	1.531 and -1.511 e.Å^{-3}

[a] $R_1 = \Sigma(||F_o| - |F_c||)/\Sigma|F_o|$. [b] $wR_2 = [\Sigma[w(F_o^2 - F_c^2)^2]/\Sigma[w(F_o^2)^2]]^{1/2}$, $w = 1/[\sigma^2(F_o^2) + [(ap)^2 + bp]$, where $p = [\max(F_o^2, 0) + 2F_c^2]/3$.

Table S2. Shape measures of the 8-coordinate Dy1 coordination polyhedra in **1**·6CH_2Cl_2, **2**·6CH_2Cl_2, **3**·2THF and **4**·2THF.

Complex	**1**·6CH_2Cl_2	**2**·6CH_2Cl_2	**3**·2THF	4·2THF
Polyhedron[a]	Dy1	Dy1	Dy2	Dy2
OP-8	28.87	28.49	28.51	29.46
HPY-8	23.62	23.66	24.07	23.16
HBPY-8	13.50	14.11	13.40	13.47
CU-8	6.73	7.81	6.23	7.75
SAPR-8	**0.99**	**0.76**	**1.10**	1.48
TDD-8	1.37	1.40	2.08	**0.94**
JGBF-8	15.31	15.63	14.98	15.53
JETBPY-8	28.07	28.19	26.81	27.51
JBTPR-8	3.06	2.83	3.22	2.86
BTPR-8	2.50	1.96	3.02	2.24
JSD-8	4.65	4.25	5.52	3.72
TT-8	7.60	8.53	7.07	8.49
ETBPY-8	23.39	23.59	23.65	23.20

[a] Abbreviations: OP-8, octagon; HPY-8, heptagonal pyramid; HBPY-8, hexagonal bipyramid; CU-8, cube; SAPR-8, square antiprism; TDD-8, triangular dodecahedron; JGBF-8, Johnson gyrobifastigium; JETBPY-8, Johnson elongated triangular bipyramid; JBTPR-8, Johnson biaugmented trigonal prism; BTPR-8, biaugmented trigonal prism; JSD-8, Johnson snub diphenoid; TT-8, triakis tetrahedron; ETBPY-8, elongated trigonal bipyramid. The values in boldface indicate the closest polyhedron according to the Continuous Shape Measures.

Magnetic measurements

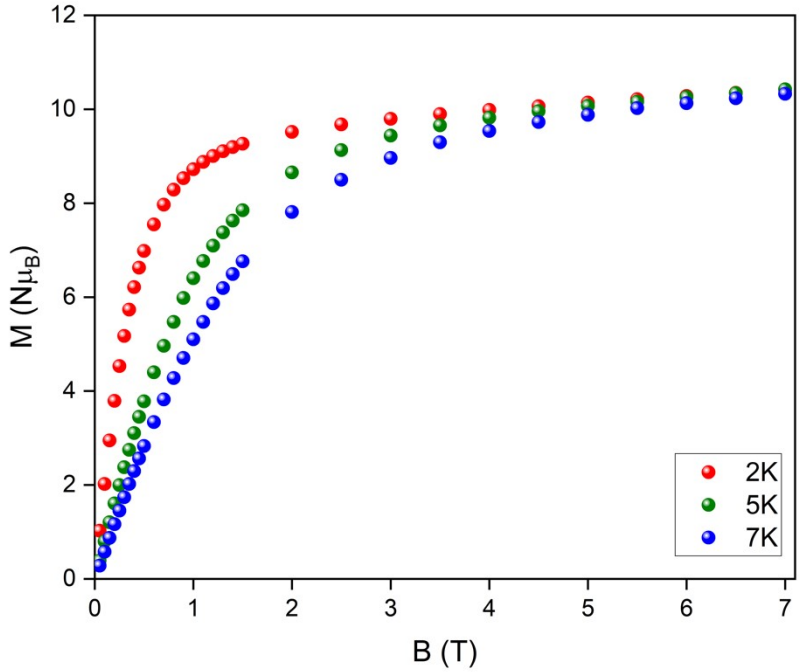

Figure S1. Magnetization (*M*) vs. magnetic field (*B*) plot for complex **1** at 2, 5 and 7 K.

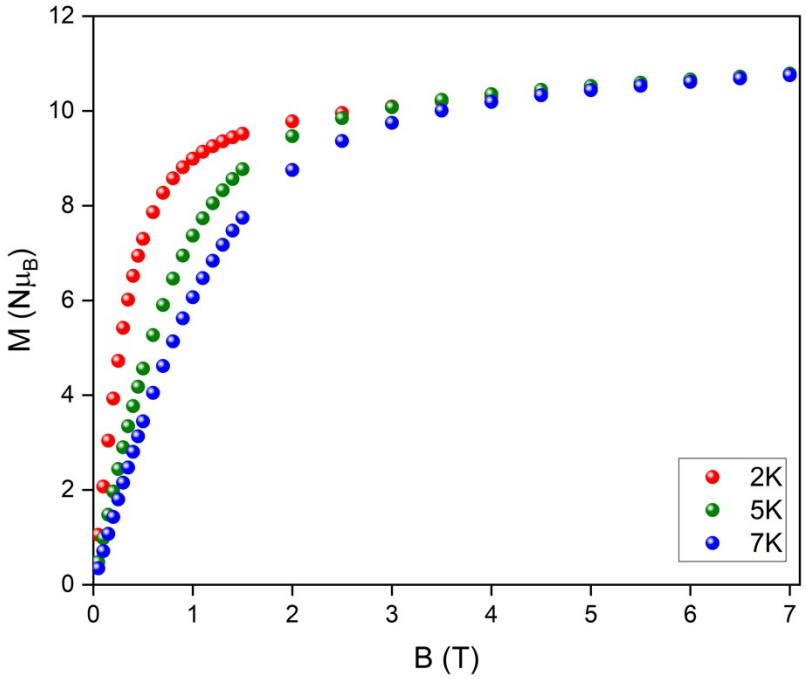

Figure S2. Magnetization (*M*) vs. magnetic field (*B*) plot for complex **2** at 2, 5, and 7 K.

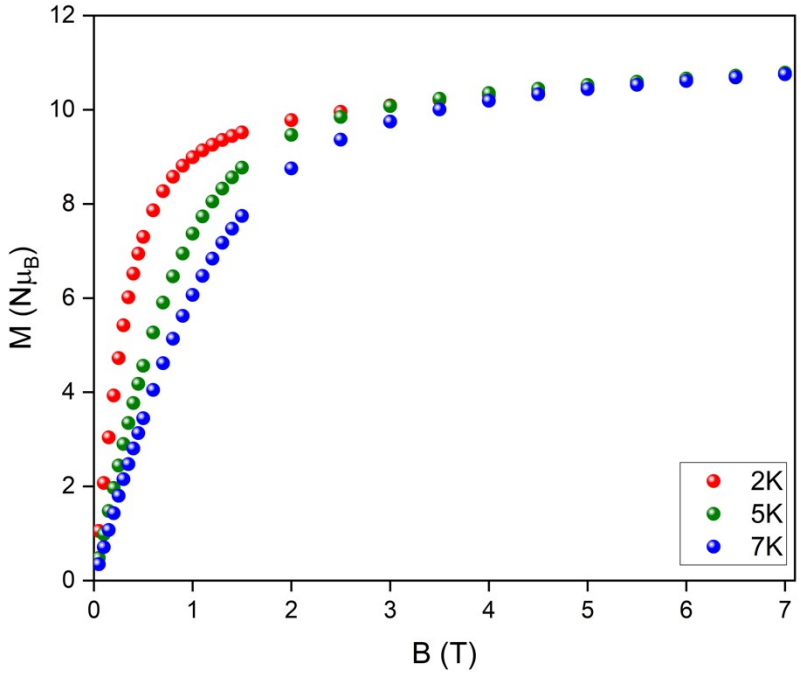

Figure S3. Magnetization (*M*) vs. magnetic field (*B*) plot for complex **3** at 2, 5 and 7 K.

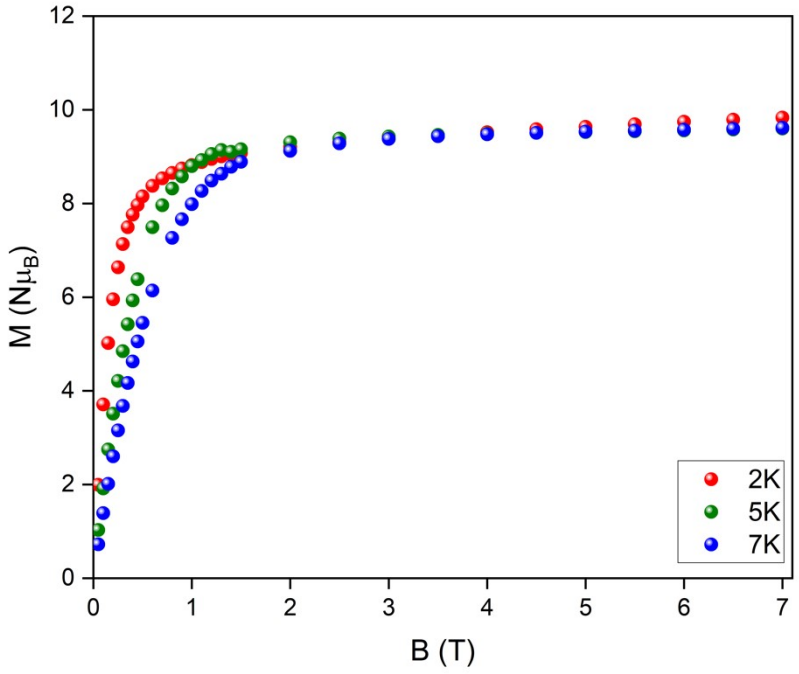

Figure S4. Magnetization (*M*) vs. magnetic field (*B*) plot for complex **4** at 2, 5 and 7 K.

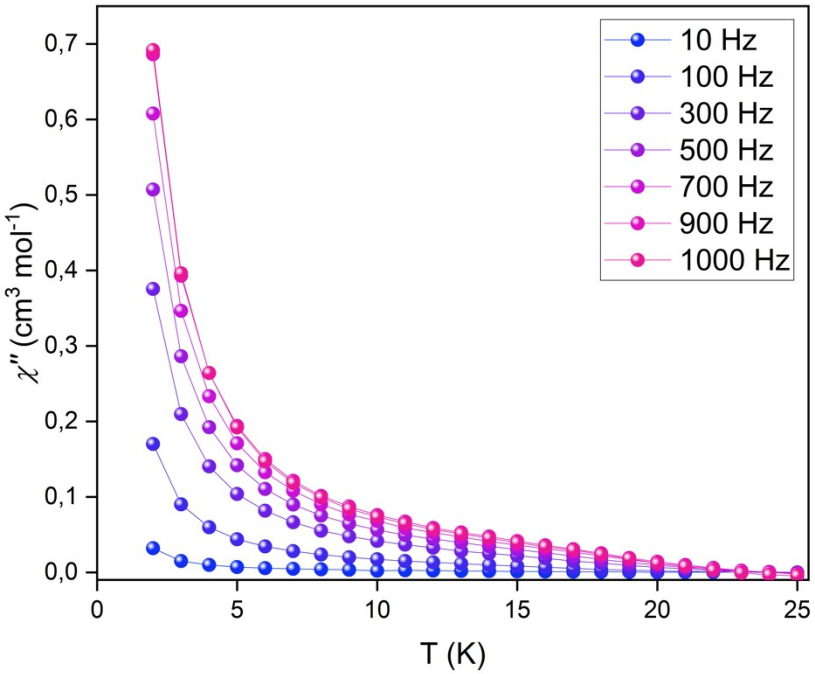

Figure S5. Temperature dependence of the out-of-phase χ'' *ac* susceptibility signals of **1** in a 2 Oe field oscillating at the indicated frequencies.

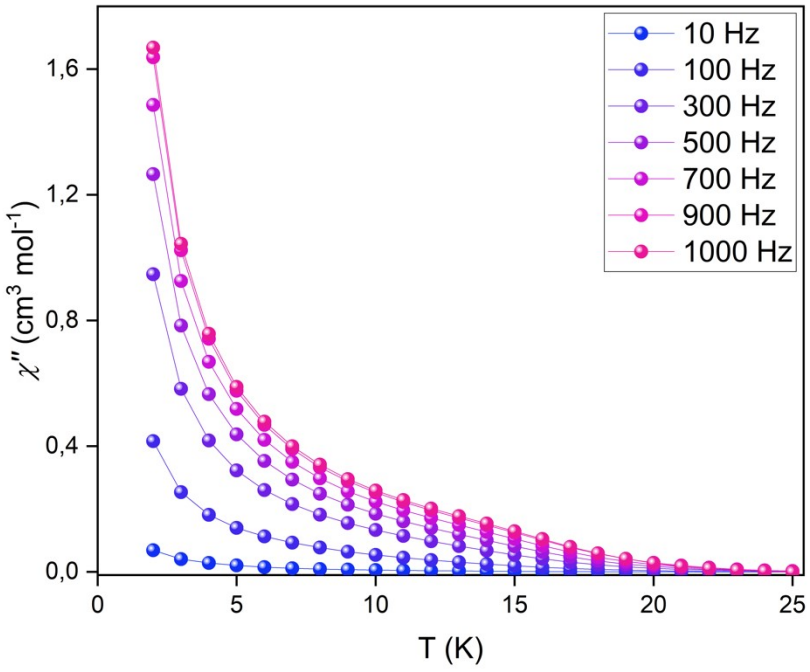

Figure S6. Temperature dependence of the out-of-phase χ'' *ac* susceptibility signals of **2** in a 2 Oe field oscillating at the indicated frequencies.

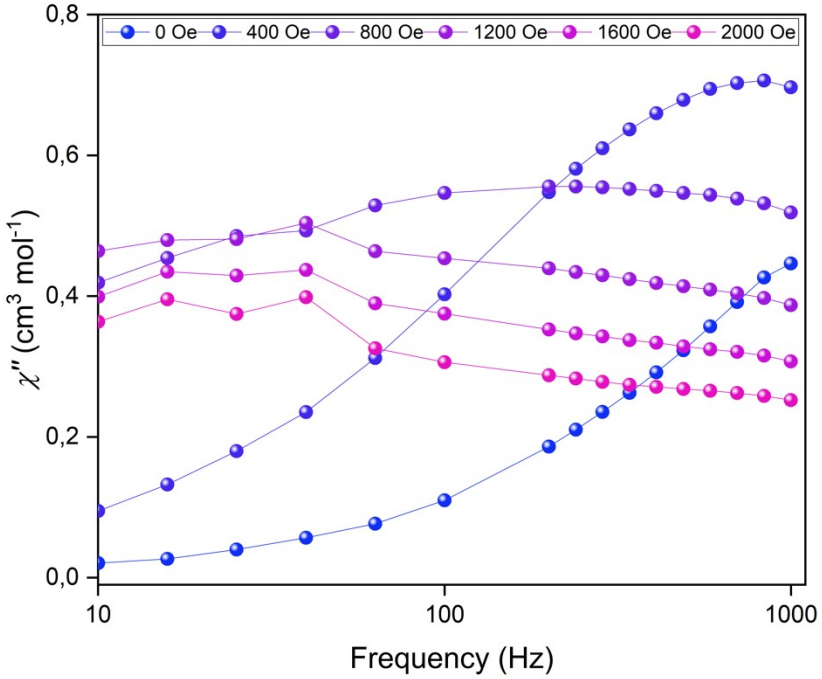

Figure S7. Out-of-phase susceptibility for **1** in various applied *dc* fields at 2 K. Solid lines are guide for the eye.

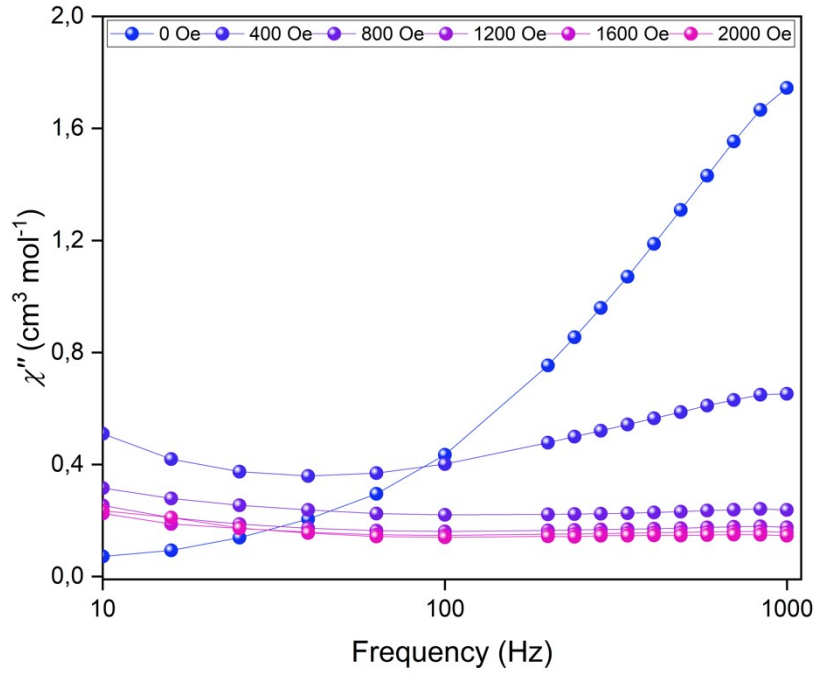

Figure S8. Out-of-phase susceptibility for **2** in various applied *dc* fields at 2 K. Solid lines are guide for the eye.

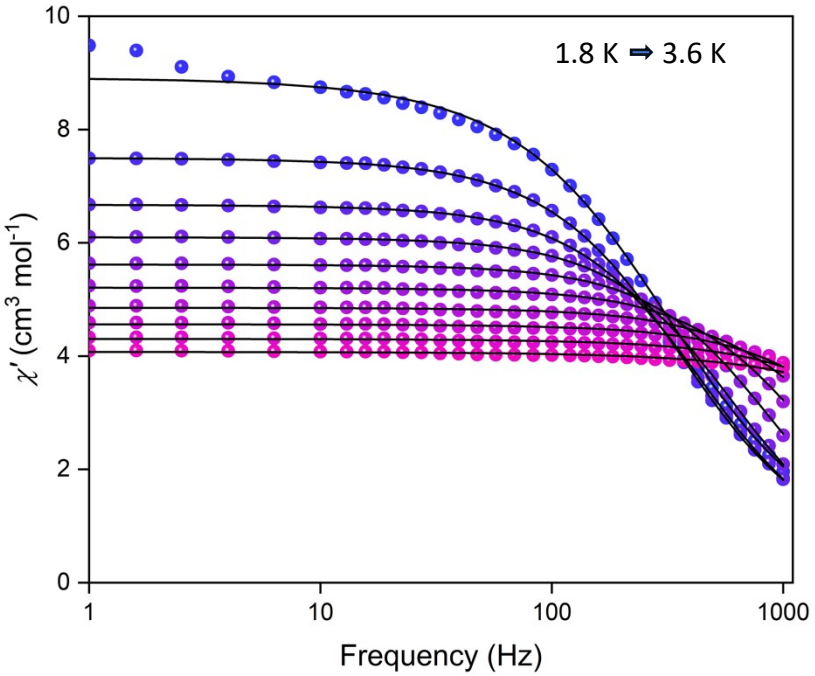

Figure S9. In-phase (χ') component of the magnetic susceptibility, under a zero Oe *dc* field, for complex **3**. Solid lines correspond to the best fit obtained with a generalized Debye model.

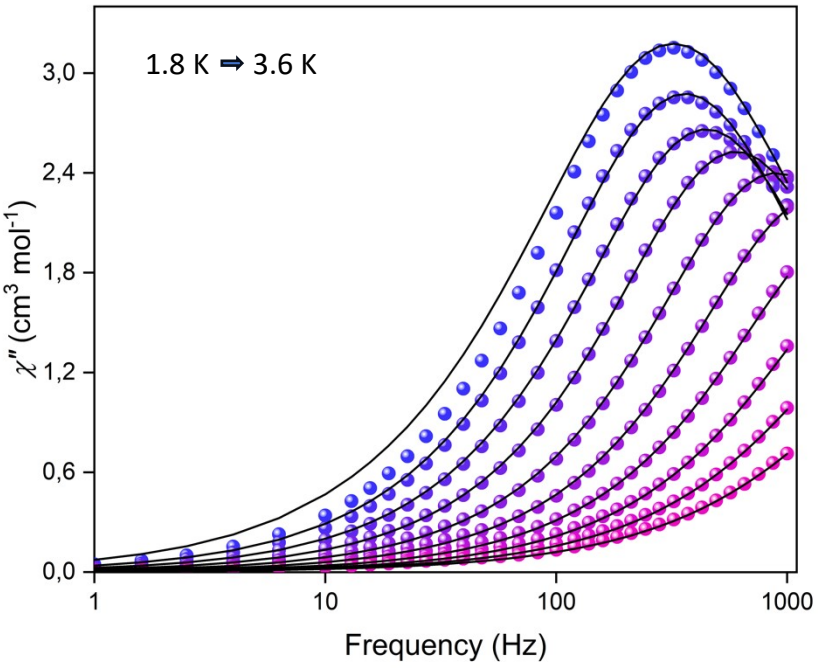

Figure S10. Out-of-phase (χ'') component of the magnetic susceptibility, under 0 Oe *dc* field, for complex **3**. Solid lines correspond to the best fit obtained with a generalized Debye model.

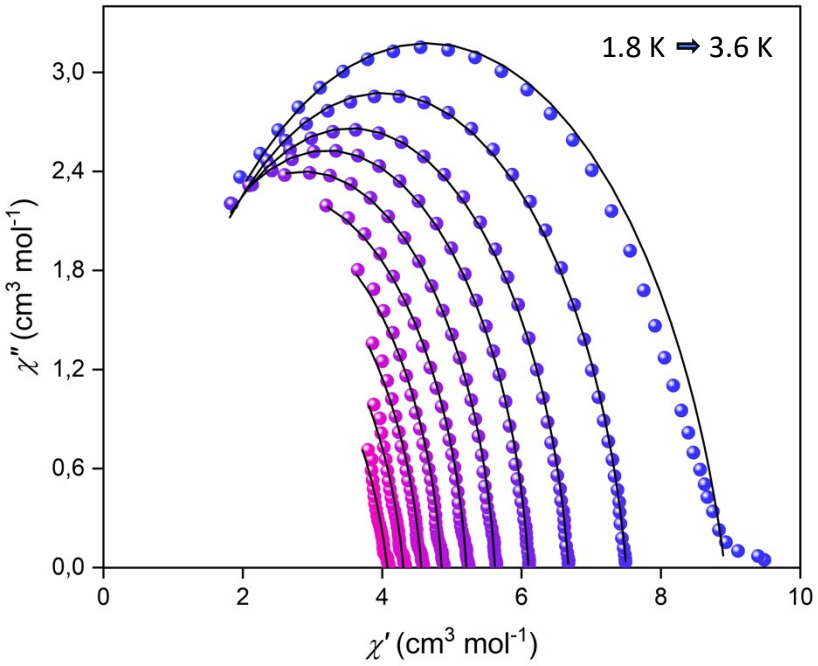

Figure S11. Cole-Cole plot for **3** obtained using the *ac* susceptibility data in a zero Oe applied *dc* field. The solid lines correspond to the best fit obtained with a generalized Debye model.

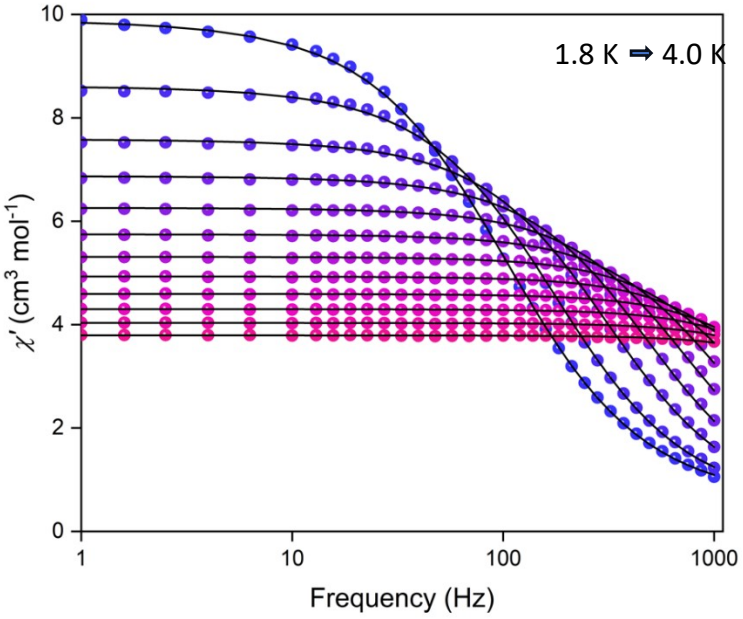

Figure S12. In-phase (χ') component of the magnetic susceptibility, under a zero Oe *dc* field, for complex **4**. Solid lines correspond to the best fit obtained with a generalized Debye model.

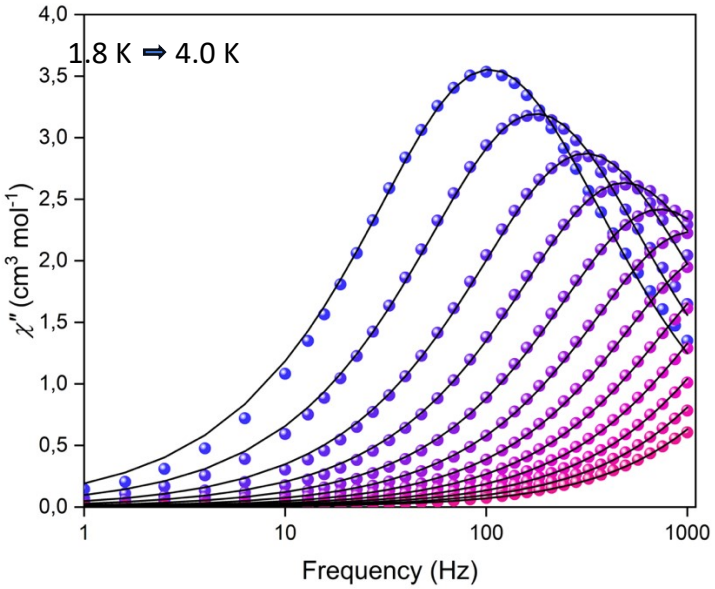

Figure S13. Out-of-phase (χ'') component of the magnetic susceptibility, under a zero Oe *dc* field, for complex **4**. Solid lines correspond to the best fit obtained with a generalized Debye model.

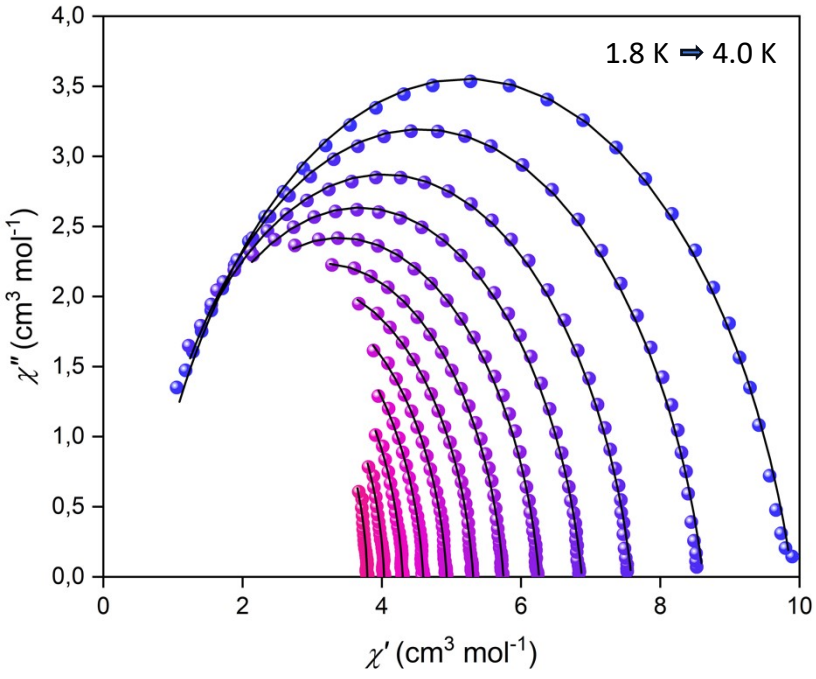

Figure S14. Cole Cole plot for **4** obtained using the *ac* susceptibility data in a zero Oe applied *dc* field. The solid lines correspond to the best fit obtained with a generalized Debye model.

Table S3. The *g*-tensor for the eight lowest Kramer's doublets in all complexes.

KDs		**1 (dhnq-neutral)**		**2 (dhaq-neutral)**		**3 (dhnq-radical)**		**4 (dhaq-radical)**	
		Dy1	Dy2	Dy1	Dy2	Dy1	Dy2	Dy1	Dy2
1	g_x	0.0473	0.0471	0.0138	0.0138	0.0690	0.0688	0.0367	0.0367
	g_y	0.0867	0.0868	0.0216	0.0217	0.0441	0.0437	0.0691	0.0691
	g_z	19.7155	19.7162	19.7806	19.7894	19.4401	19.4396	19.5550	19.5653
2	g_x	1.6177	1.6171	0.1993	0.1985	0.8102	0.8091	0.4293	0.4299
	g_y	3.0978	3.1016	0.2350	0.2348	1.4278	1.4249	0.6401	0.6405
	g_z	14.7103	14.7107	17.1069	17.0908	15.2095	15.2086	16.3432	16.3301
3	g_x	1.0287	1.0318	1.7504	1.7510	0.0108	0.0113	0.4365	0.4360
	g_y	2.2364	2.2383	2.2102	2.2093	1.5730	1.5706	1.1419	1.1435
	g_z	10.5565	10.5606	13.3562	13.3336	12.6204	12.6178	14.2391	14.2195
4	g_x	2.1855	2.1893	2.0048	2.0028	2.0302	2.0226	1.7975	1.7954
	g_y	3.2979	3.3091	3.7499	3.7444	4.6916	4.6966	3.2117	3.2102
	g_z	11.8708	11.9072	8.9215	8.9340	11.0193	11.9783	11.3599	11.3357
5	g_x	6.2726	6.2742	1.1236	1.1243	6.6363	6.6238	0.7742	0.7785
	g_y	4.9705	4.9845	6.0306	6.0291	5.0652	5.0508	3.7524	3.7540
	g_z	1.0692	1.0807	11.8172	11.8217	3.2626	3.2524	8.8352	8.8227
6	g_x	3.1380	3.1376	2.5658	2.5695	4.4214	4.4113	1.8295	1.8230
	g_y	6.2309	6.2457	3.3826	3.3881	6.3845	6.3637	6.4783	6.4894
	g_z	9.4213	9.4536	12.4365	12.4383	10.6834	10.6616	12.0180	12.0380
7	g_x	0.5997	0.5999	0.6721	0.6767	0.5890	0.5883	0.3143	0.3163
	g_y	1.4463	1.4505	1.4449	1.4478	0.7085	0.7066	0.6262	0.6252
	g_z	17.5081	17.5576	17.0148	17.0101	18.3592	18.3075	18.7383	18.7707
8	g_x	0.0035	0.0035	0.0027	0.0027	0.0109	0.0108	0.0113	0.0112
	g_y	0.0053	0.0053	0.0033	0.0033	0.0124	0.0124	0.0197	0.0196
	g_z	19.8619	19.9157	19.8907	19.8981	19.7751	19.7121	19.7067	19.6887

Table S4. RASSI energies of the lowest spin-orbit states (cm^{-1}) of each Dy center in all complexes.

1 (dhnq-neutral)		**2 (dhaq-neutral)**		**3 (dhnq-radical)**		**4 (dhaq-radical)**	
Dy1	Dy2	Dy1	Dy2	Dy1	Dy2	Dy1	Dy2
0.000	0.000	0.000	0.000	0.000	0.000	0.000	0.000
0.000	0.000	0.000	0.000	0.000	0.000	0.000	0.000
148.129	148.129	149.669	149.669	154.412	154.411	157.799	157.803
148.129	148.129	149.669	149.669	154.412	154.411	157.799	157.803
195.430	195.430	261.886	261.882	241.350	241.354	248.610	248.632
195.430	195.430	261.886	261.882	241.350	241.354	248.610	248.632
226.131	226.131	313.572	313.562	318.936	318.947	326.219	326.279
226.131	226.131	313.572	313.562	318.936	318.947	326.219	326.279
255.741	255.741	329.679	329.675	338.812	338.821	389.904	389.992
255.741	255.741	329.679	329.675	338.812	338.821	389.904	389.992
286.674	286.673	346.360	346.356	383.286	383.294	428.302	428.421
286.674	286.673	346.360	346.356	383.286	383.294	428.302	428.421
330.447	330.446	378.725	378.719	464.819	464.841	493.070	493.204
330.447	330.446	378.725	378.719	464.819	464.841	493.070	493.204
641.637	641.637	697.301	697.301	740.217	740.224	740.648	740.743
641.637	641.637	697.301	697.301	740.217	740.224	740.648	740.743
3064.370	3064.370	3055.314	3055.313	3083.683	3083.686	3067.831	3067.828
3064.370	3064.370	3055.314	3055.313	3083.683	3083.686	3067.831	3067.828
3104.656	3104.656	3158.315	3158.314	3132.971	3132.975	3156.669	3156.695
3104.656	3104.656	3158.315	3158.314	3132.971	3132.975	3156.669	3156.695
3186.245	3186.245	3232.266	3232.262	3243.216	3243.223	3265.408	3265.464
3186.245	3186.245	3232.266	3232.262	3243.216	3243.223	3265.408	3265.464
3230.629	3230.629	3297.473	3297.467	3317.889	3317.900	3343.369	3343.443
3230.629	3230.629	3297.473	3297.467	3317.889	3317.900	3343.369	3343.443
3250.546	3250.546	3313.941	3313.931	3364.650	3364.668	3402.843	3402.944
3250.546	3250.546	3313.941	3313.931	3364.650	3364.668	3402.843	3402.944
3331.578	3331.578	3389.312	3389.311	3426.188	3426.200	3446.181	3446.286
3331.578	3331.578	3389.312	3389.311	3426.188	3426.200	3446.181	3446.286
3449.941	3449.941	3511.598	3511.598	3542.803	3542.811	3547.711	3547.804
3449.941	3449.941	3511.598	3511.598	3542.803	3542.811	3547.711	3547.804
5661.700	5661.700	5674.104	5674.103	5703.265	5703.269	5685.856	5685.865
5661.700	5661.700	5674.104	5674.103	5703.265	5703.269	5685.856	5685.865
5689.382	5689.382	5739.989	5739.986	5720.051	5720.057	5758.780	5758.830
5689.382	5689.382	5739.989	5739.986	5720.051	5720.057	5758.780	5758.830
5772.280	5772.280	5826.987	5826.981	5840.399	5840.409	5867.234	5867.296
5772.280	5772.280	5826.987	5826.981	5840.399	5840.409	5867.234	5867.296
5817.638	5817.638	5878.781	5878.772	5925.072	5925.089	5954.614	5954.710
5817.638	5817.638	5878.781	5878.772	5925.072	5925.089	5954.614	5954.710
5921.855	5921.855	5955.284	5955.284	5990.983	5990.992	5998.423	5998.497
5921.855	5921.855	5955.284	5955.284	5990.983	5990.992	5998.423	5998.497

5948.264	5948.264	6027.457	6027.456	6053.512	6053.525	6068.113	6068.206
5948.264	5948.264	6027.457	6027.456	6053.512	6053.525	6068.113	6068.206
7846.907	7846.907	7877.234	7877.232	7890.577	7890.583	7891.384	7891.400
7846.907	7846.907	7877.234	7877.232	7890.577	7890.583	7891.384	7891.400
7879.564	7879.564	7926.760	7926.757	7924.634	7924.643	7955.949	7956.013
7879.564	7879.564	7926.760	7926.757	7924.634	7924.643	7955.949	7956.013
7974.170	7974.169	8031.531	8031.523	8063.104	8063.118	8087.905	8087.984
7974.170	7974.169	8031.531	8031.523	8063.104	8063.118	8087.905	8087.984
8078.262	8078.262	8104.811	8104.809	8146.685	8146.695	8153.339	8153.409
8078.262	8078.262	8104.811	8104.809	8146.685	8146.695	8153.339	8153.409
8096.870	8096.870	8179.551	8179.549	8200.361	8200.375	8219.789	8219.880
8096.870	8096.870	8179.551	8179.549	8200.361	8200.375	8219.789	8219.880
9586.842	9586.842	9627.076	9627.073	9630.686	9630.693	9643.084	9643.119
9586.842	9586.842	9627.076	9627.073	9630.686	9630.693	9643.084	9643.119
9623.344	9623.344	9661.127	9661.123	9679.742	9679.755	9692.339	9692.393
9623.344	9623.344	9661.127	9661.123	9679.742	9679.755	9692.339	9692.393
9639.996	9639.996	9683.787	9683.785	9706.111	9706.124	9720.176	9720.245
9639.996	9639.996	9683.787	9683.785	9706.111	9706.124	9720.176	9720.245
9653.019	9653.019	9709.819	9709.816	9718.195	9718.208	9740.400	9740.463
9653.019	9653.019	9709.819	9709.816	9718.195	9718.208	9740.400	9740.463
9688.082	9688.082	9741.642	9741.638	9758.375	9758.387	9780.759	9780.824
9688.082	9688.082	9741.642	9741.638	9758.375	9758.387	9780.759	9780.824
9718.061	9718.061	9769.792	9769.786	9801.268	9801.284	9818.730	9818.802
9718.061	9718.061	9769.792	9769.786	9801.268	9801.284	9818.730	9818.802
9749.413	9749.413	9798.698	9798.694	9825.056	9825.070	9841.600	9841.678
9749.413	9749.413	9798.698	9798.694	9825.056	9825.070	9841.600	9841.678
9812.125	9812.125	9854.822	9854.819	9895.382	9895.395	9908.024	9908.105
9812.125	9812.125	9854.822	9854.819	9895.382	9895.395	9908.024	9908.105
9860.816	9860.816	9898.419	9898.417	9945.447	9945.461	9951.299	9951.374
9860.816	9860.816	9898.419	9898.417	9945.447	9945.461	9951.299	9951.374
9901.458	9901.458	9969.863	9969.861	9999.093	9999.108	……..	……..
9901.458	9901.458	9969.863	9969.861	9999.093	9999.108		
…….	……	…….	……	……..	……..		

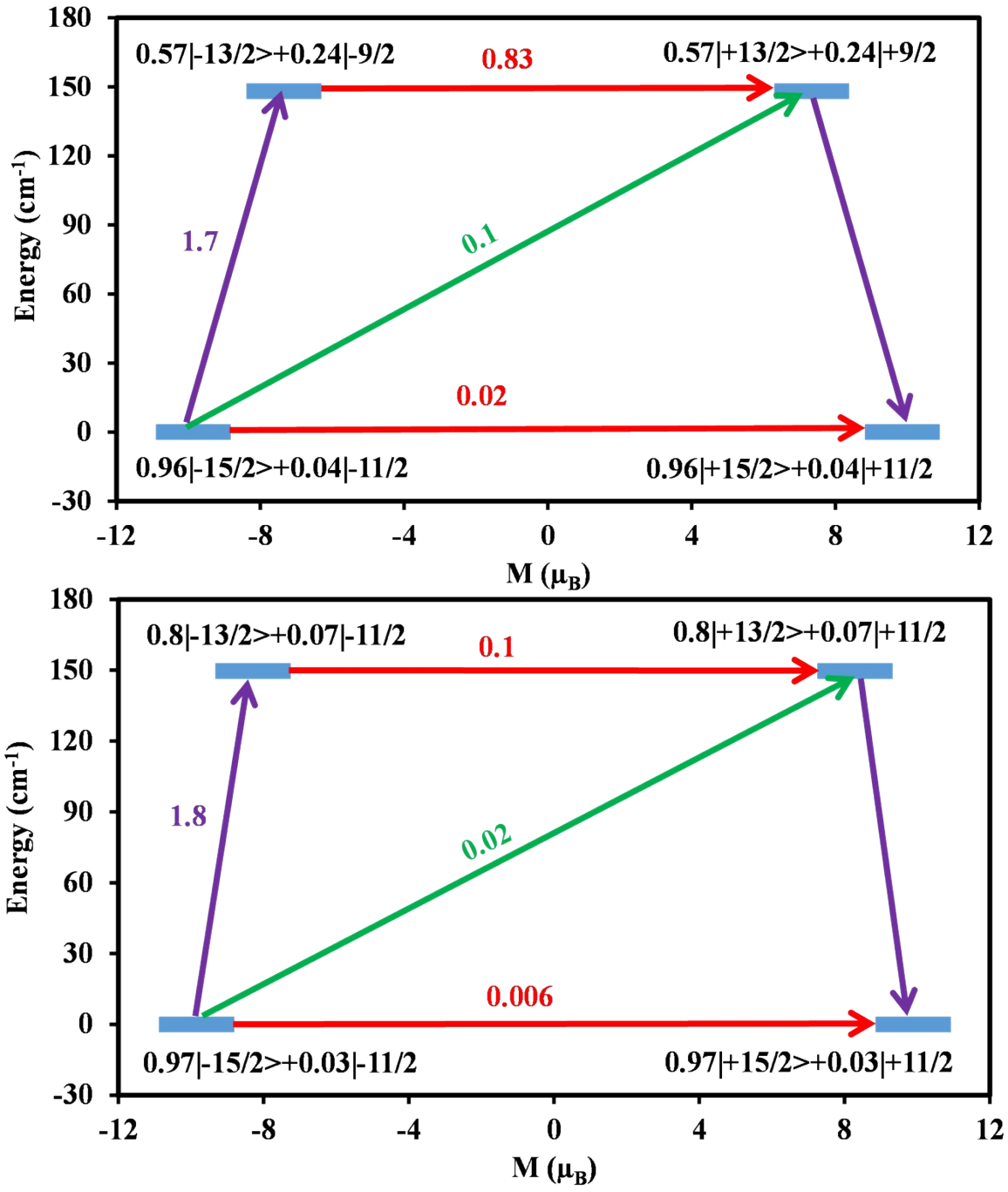

Figure S15. *Ab initio* computed magnetization blocking barrier for Dy1 site (same applicable for Dy2 site) in (top) **1**, and (bottom) **2**. The thick blue line indicates the Kramers doublets (KDs) as a function of computed magnetic moment. The red arrows represent the presence of QTM/TA-QTM between the connecting pairs. The green/purple arrows show the possible pathway via Orbach/Raman relaxation. The numbers provided at each arrow are the mean absolute value for the corresponding matrix element of the transition magnetic moment.

Table S5. SINGLE_ANISO computed crystal field parameters for all complexes. The major components in the Table are in bold. B_k^q is the crystal field parameter and O_k^q is the extended Stevens operator. The quantization axis is chosen to be the main magnetic axis of the ground pseudo-doublet.

k	q	B_k^q	B_k^q	B_k^q	B_k^q	B_k^q	B_k^q	B_k^q	B_k^q
		1 (dhnq-neutral)		**2 (dhaq-neutral)**		**3 (dhnq-radical)**		**4 (dhaq-radical)**	
		Dy1	Dy2	Dy1	Dy2	Dy1	Dy2	Dy1	Dy2
2	-2	-1.98	-1.98	-1.91	-1.91	-2.02	-2.02	1.50	1.50
	-1	0.38	0.38	0.82	0.85	-0.02	-0.03	0.94	0.82
	0	**-2.05**	**-2.05**	**-2.54**	**-2.54**	**-2.73**	**-2.73**	**-2.97**	**-2.97**
	1	0.57	0.57	-0.58	-0.58	-0.39	-0.44	-1.47	-1.62
	2	-0.17	-0.18	0.11	0.11	0.69	0.70	0.50	0.49
4	-4	0.02	0.02	0.01	0.01	0.02	0.02	-0.02	-0.02
	-3	0.02	0.02	0.03	0.03	-0.003	-0.003	0.02	0.02
	-2	0.03	0.03	0.01	0.02	0.02	0.03	-0.02	-0.02
	-1	0.001	0.001	-0.02	-0.02	0.0002	0.0001	-0.01	-0.01
	0	-0.0003	-0.0003	-0.002	-0.002	0.0008	0.0008	0.0006	0.0006
	1	0.0007	0.0007	0.02	0.02	0.0008	0.0005	-0.008	-0.007
	2	0.02	0.02	0.01	0.01	0.03	0.03	0.03	0.03
	3	0.0002	0.0002	0.05	0.05	-0.001	-0.005	-0.04	-0.04
	4	-0.02	-0.02	-0.02	-0.02	-0.01	-0.01	-0.01	-0.01
6	-6	3×10^{-4}	3×10^{-4}	3×10^{-4}	3×10^{-4}	1×10^{-4}	1×10^{-4}	-9×10^{-5}	-1×10^{-6}
	-5	-8×10^{-5}	-8×10^{-5}	-5×10^{-4}	-5×10^{-4}	5×10^{-5}	5×10^{-5}	-3×10^{-4}	-3×10^{-4}
	-4	-3×10^{-5}	-3×10^{-5}	-4×10^{-5}	-4×10^{-5}	-8×10^{-5}	-8×10^{-5}	7×10^{-5}	7×10^{-5}
	-3	1×10^{-5}	2×10^{-5}	-1×10^{-4}	-1×10^{-4}	1×10^{-5}	4×10^{-6}	-8×10^{-5}	-7×10^{-5}
	-2	-2×10^{-4}	-2×10^{-4}	2×10^{-5}	2×10^{-5}	-3×10^{-4}	-3×10^{-4}	2×10^{-4}	2×10^{-4}
	-1	-5×10^{-5}	-5×10^{-5}	2×10^{-4}	2×10^{-4}	-2×10^{-6}	-2×10^{-6}	2×10^{-4}	1×10^{-4}
	0	-4×10^{-5}	-4×10^{-5}	-8×10^{-6}	-8×10^{-6}	-4×10^{-5}	-4×10^{-5}	-3×10^{-5}	-3×10^{-5}
	1	-6×10^{-5}	-5×10^{-5}	-3×10^{-4}	-3×10^{-4}	2×10^{-5}	2×10^{-5}	3×10^{-4}	3×10^{-4}
	2	4×10^{-6}	3×10^{-6}	8×10^{-5}	8×10^{-5}	-2×10^{-6}	-2×10^{-6}	1×10^{-5}	1×10^{-5}
	3	-3×10^{-6}	-3×10^{-6}	-2×10^{-4}	-2×10^{-4}	-3×10^{-5}	-3×10^{-5}	2×10^{-4}	2×10^{-4}
	4	-7×10^{-6}	-8×10^{-6}	-3×10^{-6}	-4×10^{-6}	-7×10^{-5}	-7×10^{-5}	-4×10^{-5}	-4×10^{-5}
	5	-3×10^{-5}	-3×10^{-5}	5×10^{-4}	5×10^{-4}	4×10^{-5}	3×10^{-5}	1×10^{-5}	1×10^{-5}
	6	3×10^{-4}	3×10^{-4}	1×10^{-4}	1×10^{-4}	3×10^{-4}	3×10^{-4}	3×10^{-4}	3×10^{-4}

Table S6. Lowest exchange coupled doublets (cm^{-1}) arising from the dipolar coupling, the corresponding tunnel splitting (Δ_{tun}, cm^{-1}), and the g_z value of each doublet (g_x and $g_y \neq 0$) for complex **1 (dhnq-neutral)**.

No.	E(cm^{-1})	Δ_{tun}	g_z
1	0.000000000000 0.000013117958	1.3×10^{-5}	0.009014538
2	0.14151752112 0.14158289857	6.5×10^{-5}	39.431592335
3	148.130878851390 148.131243950245	3.7×10^{-4}	0.015966622
4	148.165567044237 148.166119477402	5.5×10^{-4}	0.016585500
5	148.214882393171 148.215219180049	3.4×10^{-4}	34.387253854

Table S7. Lowest exchange-coupled doublets (cm^{-1}) arising from the dipolar coupling, the corresponding tunnel splitting (Δ_{tun}, cm^{-1}), and the g_z value of each doublet (g_x and $g_y \neq 0$) for complex **2 (dhaq-neutral)**.

No.	E(cm^{-1})	Δ_{tun}	g_z
1	0.000000000000 0.000072068548	7.2×10^{-5}	0.015119101
2	0.000273569492 0.000345903879	7.2×10^{-5}	35.186731528
3	149.654310247509 149.654343934220	3.7×10^{-5}	0.067301954
4	149.659334902398 149.659383720067	4.9×10^{-5}	0.063365989
5	149.67059706569 149.67078980861	1.9×10^{-4}	36.463776932

Table S8. Lowest exchange coupled doublets (cm^{-1}) arising from the dipolar coupling, the corresponding tunnel splitting (Δ_{tun}, cm^{-1}), and the g_z value of each doublet (g_x and $g_y \neq 0$) for complex **3 (dhnq-radical)**.

No.	E(cm^{-1})	Δ_{tun}	g_z
1	0.000000000000 0.000000000443	4.4×10^{-10}	1.877125805
2	19.056141497248 19.056141498581	1.3×10^{-9}	38.394173265
3	19.058833239414	1.4×10^{-9}	5.056315171

	19.058833240772		
4	24.575113133233 24.575113133383	1.5 x 10^{-10}	34.015569958
5	156.122916506415 156.122916506610	2.0 x 10^{-10}	7.062910997
6	157.210465818809 157.210465819263	4.5 x 10^{-10}	33.940841436
7	170.956097140521 170.956097140695	1.7 x 10^{-10}	7.273650403
8	170.984845602749 170.984845602937	1.9 x 10^{-10}	31.768419947
9	174.220752195111 174.220752195431	3.2 x 10^{-10}	6.790325100
10	174.2239204831511 74.223920483405	2.5 x 10^{-10}	32.177365219

Table S9. Lowest exchange coupled doublets (cm^{-1}) arising from the dipolar coupling, the corresponding tunnel splitting (Δ_{tun}, cm^{-1}), and the g_z value of each doublet (g_x and $g_y \neq 0$) for complex **4 (dhaq-radical)**.

No.	E(cm^{-1})	Δ_{tun}	g_z
1	0.000000000000 0.000000000051	5.1 x 10^{-11}	37.130207397
2	5.624669918197 5.624669918211	1.4 x 10^{-11}	41.123456726
3	10.190201796891 10.190201796946	5.5 x 10^{-11}	1.914837637
4	10.190540545425 10.190540545490	6.5 x 10^{-11}	1.918929007
5	158.113790442647 158.113790442871	2.2 x 10^{-10}	33.738112998
6	159.388117689533 159.388117689933	4.0 x 10^{-10}	33.750329356
7	163.263636288134 163.263636288209	7.5 x 10^{-10}	37.726842693
8	164.524646689670 164.524646689916	2.5 x 10^{-10}	37.739286781

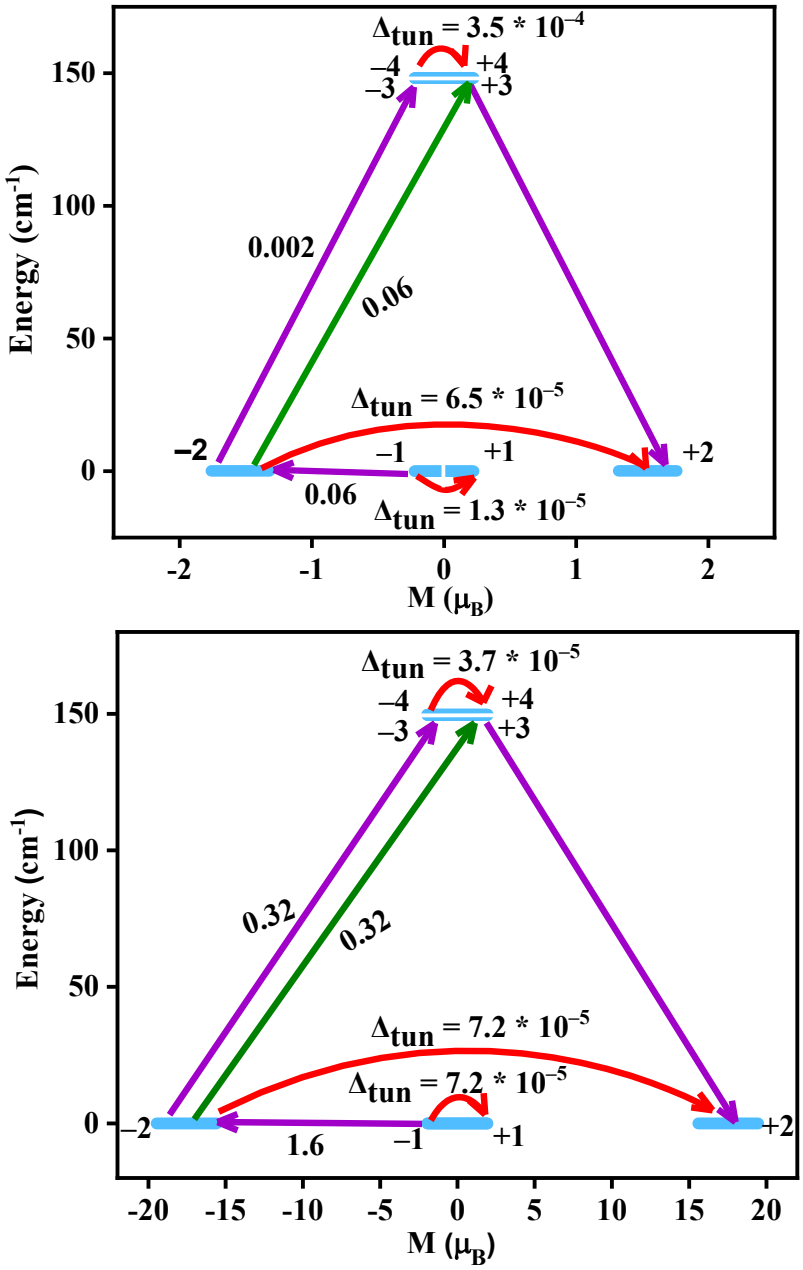

Figure S16. Low-lying exchange spectra in (top) **1 (dhnq-neutral)**, and (bottom) **2 (dhaq-neutral)**. The exchange-coupled states are placed on the diagram according to their magnetic moments (bold blue lines). The red arrows show the tunneling gap within each doublet state, while the green/purple arrows show the possible spin–phonon transitions. The numbers provided at each arrow are the mean absolute value for the corresponding matrix element of the transition magnetic moment.